

Electronic structure of La-intercalated graphite

A. M. Shikin,* S. L. Molodtsov,*[†] C. Laubschat,[†] and G. Kaindl

Institut für Experimentalphysik, Freie Universität Berlin, Arnimallee 14, D-14195 Berlin-Dahlem, Germany

G. V. Prudnikova and V. K. Adamchuk

Institute of Physics, St. Petersburg State University, 198904 St. Petersburg, Russia

(Received 30 December 1994)

We demonstrate that a graphite-intercalation compound (GIC) with La is formed when an 80-Å-thick film of La metal deposited onto highly oriented pyrolytic graphite is annealed at temperatures between 400 and 1200°C. The resulting intercalation compound was studied by angle-resolved photoemission, Auger-electron spectroscopy, and low-energy-electron diffraction. It was found that despite differences in the electronic configurations of La metal (*d* metal) and alkali metals (*s* metals), the valence-band structure of the obtained La-GIC is quite similar to that of alkali-GIC. It is proposed that the electronic structure of the La-GIC can be described in first approximation by a rigid-band model, where the valence electrons of La are preferentially transferred to the graphite p_{π^*} band and not so much to states of the three-dimensional interlayer band.

INTRODUCTION

In the recent past, graphite intercalation compounds (GIC's) have been the subject of numerous experimental and theoretical studies due to their interesting structural, electronic, and transport properties.¹⁻⁸ These compounds consist of stacks of one or more layers of hexagonally arranged carbon atoms (graphite layers) that alternate with ordered monolayers of intercalated atoms, molecules, or radicals. The weak van der Waals forces that are characteristic of bonding between neighboring planes in the quasi-two-dimensional structure of graphite allow the incorporation of a wide variety of intercalants with widely varying sizes between the graphite planes. The spacing between adjacent carbon layers can range from 3.35 Å up to ≈ 8 Å to allow the accommodation of an intercalant layer.¹ Such a layered structure gives rise to well-defined anisotropies in the electrical and electronic properties of these materials.

Until now alkali-metal GIC's, which can be easily grown *in situ* in ultrahigh vacuum (UHV), have attracted the main spectroscopic interest due to their fascinating properties including two-dimensional superconductivity.^{9,10} Semiempirical tight-binding and pseudopotential calculations^{11,12} have predicted that a significant fraction of the *s* electrons from the alkali atoms remains in alkali-derived metallic states. Subsequent work^{3,13} claimed that these compounds are characterized by an almost complete charge transfer of valence electrons from the alkali atoms to p_{π^*} unoccupied states of graphite. However, inverse photoemission^{14,15} as well as x-ray-absorption near-edge structure¹⁶ studies showed that such a simplistic model is complicated by the presence of a three-dimensional interlayer band that is located above the Fermi level (E_F) around the Γ point of the Brillouin zone (BZ) in pristine graphite.¹⁷ Upon intercalation, charge transfer leads to a lowering of this band, which for alkali-GIC has a minimum below E_F . This implies sub-

stantial *s* character at the Fermi level, as predicted in the early calculations.^{11,12}

The interest in low-dimensional magnetism has resulted in a number of studies of magnetic GIC's.^{4,18} Since the atomic positions of intercalant atoms are virtually fixed to the space between the centers of two C hexagons in neighboring graphite planes,¹⁹ a unique opportunity for growing well-ordered magnetic multilayer structures arises. The lanthanide elements (Ln) are very promising candidates for magnetic GIC's. The large ionic radii of Ln are expected to lead to rather slow diffusion and hence to a high stability of the resulting GIC's.²⁰ If a method could be found to prepare lanthanide-intercalation compounds (Ln-GIC), it would allow one to change the distance between neighboring magnetic layers in a graphite matrix leading to variations in the strength of magnetic coupling between the neighboring Ln layers. The interest in these GIC's arises from both possible technological applications and a fundamental interest in studying the similarities and differences in chemical bonding in *s*- and *d*-metal-derived GIC's. Until recently, studies of the electronic structure of Ln-GIC's by spectroscopic methods were complicated by the difficult procedure for growing these species *in situ*, in particular due to the chemically active *d* shell, which can lead to the destruction of the graphite sp^2 hybrids and to the formation of carbidelike phases.^{20,21}

In the present paper we report on an angle-resolved photoemission (PE), Auger-electron spectroscopy (AES), and low-energy-electron diffraction (LEED) study of highly oriented pyrolytic graphite (HOPG) intercalated *in situ* with La. The method applied for *in situ* intercalation by La includes destruction of the outermost C planes by annealing the La-HOPG interface at 400–900°C in order to obtain an intermixed surface phase of La carbide. Further annealing at higher temperatures ($\approx 1200^\circ\text{C}$) intensifies the interdiffusion between La and C, resulting in a C-enriched surface layer and a recover-

ing of hexagonal graphite planes due to the orienting role of the graphite substrate. Present results on the electronic structure of this surface compound formed on HOPG demonstrate a striking similarity with that of alkali-intercalated graphite.

EXPERIMENTAL DETAILS

Highly oriented pyrolytic graphite (obtained from Union Carbide) was used as the host matrix for intercalation with La. The dimensions of the HOPG wafers were typically $10 \times 7 \times 0.7 \text{ mm}^3$. These wafers were cleaved with the help of a tape glued onto their surfaces, and subsequently annealed *in situ* for several hours at a temperature of $\approx 1400^\circ\text{C}$ in a vacuum better than 3×10^{-10} mbar; in this way, the HOPG wafers were depleted of possible bulk contaminants. The HOPG substrates cleaned in this way revealed a LEED pattern with a series of concentric rings that contained tracing spots originating from the reciprocal lattice of graphite. The location of these spots on the rings varied with the position of the electron beam on the surface, an observation that points to sizes of the monocrystalline domains of the order of the diameter of the electron beam.

In situ intercalation of La into graphite was achieved by thermal deposition of a thick La layer ($\approx 80 \text{ \AA}$ thick) onto the graphite substrate, followed by a cycle of annealing at various temperatures. La metal was evaporated from a bead molten on a thin W-Re wire; the pressure in the experimental chamber was always better than 1×10^{-10} mbar during evaporation. The thickness of the deposited lanthanum layer was monitored by a quartz microbalance. Step-by-step annealing at increasing temperatures in the range from 400 to 1200°C , with intervals of 100°C and annealing periods of 5 min each, resulted in an ordered compound that is characterized by a LEED pattern similar to that of graphite. The LEED patterns show some additional rings arising from a locally reconstructed surface of the La-GIC.

Angle-resolved PE measurements were performed with an ARIES spectrometer (from Vacuum Science Workshop, Ltd.) at the Berliner Elektronenspeicherring für Synchrotronstrahlung (BESSY) using monochromatic light from the TGM5 undulator beamline, which is equipped with a toroidal-grating monochromator. The overall system resolution was about 100 meV [full width at half maximum (FWHM)]. Valence-band PE spectra of the clean HOPG substrate and the La-intercalated compounds were taken with 50-eV photons. An AES study was carried out in a separate experimental setup exploiting a four-grid LEED optics with an energy resolution of 0.2%, using a 1-keV primary electron beam with 0.3-eV amplitude modulation.

EXPERIMENTAL RESULTS

The AES spectra taken in dN/dE mode in the region of the C(KVV) Auger signal are shown in Fig. 1 for pristine HOPG as well as for the La-carbon compounds obtained after annealing at various temperatures. The shape of the AES spectrum of HOPG is similar to the results reported in literature.^{22,23} In difference to the spec-

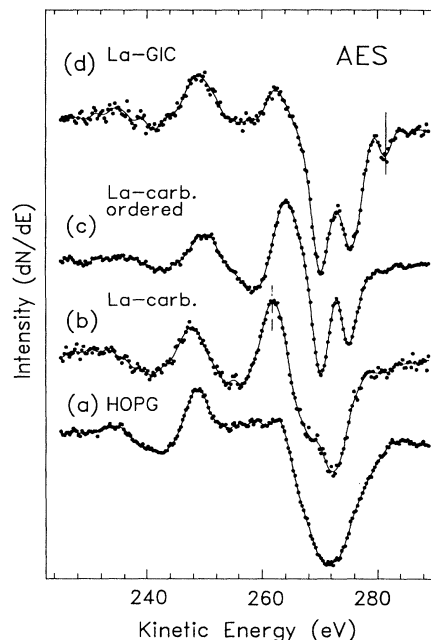


FIG. 1. C(KVV) AES spectra recorded in the dN/dE mode: (a) HOPG, (b) nonordered, and (c) ordered phases of La carbides, (d) La-intercalated HOPG.

trum for clean HOPG [Fig. 1(a)], the C(KVV) Auger signal from the La/graphite interface after annealing at temperatures between 400 and 600°C [Fig. 1(b)] exhibits a well-pronounced shoulder at 269 eV and an enhanced feature at 262 eV (dashed vertical bar). The corresponding spectrum taken in the $N(E)$ mode (Ref. 21; not shown here) is characterized by a triplet structure in the region 230–276 eV. Similar structures from C(KVV) Auger transitions involving valence electrons have previously been observed for carbides of d transition metals.^{23,24} These features can be described as due to a convolution of C $2s$ states with C $2p$ -metal d valence-band hybrids, which are characteristic for carbides. The presence of the discussed structures in the spectra [e.g., Fig. 1(b)] is interpreted as a signature of carbide formation after these low-temperature annealing steps. This phase is not ordered, however, since no LEED pattern could be observed. The in-plane sp^2 hybrid bonds of graphite have been destroyed in this phase, leading to an intermixing of La and C atoms.

Annealing of the La-graphite interface at temperatures up to $\approx 900^\circ\text{C}$ leads to further pronounced changes in the shape of the C(KVV) Auger signal [Fig. 1(c)]. Apart from a shift of the whole structure toward higher kinetic energies, the main feature at 272 eV splits into two minima at energies of 270 and 275 eV, respectively. Annealing at such moderate temperatures results in an ordering of the La-carbide film as was monitored by LEED. Further annealing at temperatures between 1000 and 1200°C changes the spectral shape in the high-energy region [Fig. 1(d)]. An interesting sharp feature (marked by the solid vertical bar) appears at about 281 eV. On the other hand, the 262-eV structure, characteristic of the carbide phase,

loses intensity and the whole spectrum shifts back to lower energies. The LEED pattern for this phase is similar to that for pyrolytic graphite modified by an additional series of smooth rings. This latter observation is in agreement with structural studies^{19,25} that have demonstrated a reconstruction of the graphite surface upon intercalation with alkali metals.

A similar shape of the C(*KVV*) AES signal, with a rather sharp feature in the high-energy region, has been observed for alkali-GIC.²⁶ The high-kinetic-energy peak can be assigned within the framework of the rigid-band model. Due to the charge transfer of valence electrons from the metal to carbon sites, the unoccupied states of C are shifted below the Fermi level; they appear in the self-convolution of the C-derived valence-band states reflected in the C(*KVV*) Auger signal. As calculated for GIC's,⁶ the charge is mainly transferred to p_{π^*} electronic states of carbon, which are placed in a region around the *K* point at the border of the BZ of graphite. Since the Auger process leads to an averaging of the signal in *k* space, the charge-transfer feature in the C(*KVV*) signal is not as intense as has been observed for alkali-GIC's in angle-resolved PE spectra taken at an angle corresponding to the *K* point.⁷

Surface-sensitive angle-resolved PE spectra of HOPG and of the various La-C phases, taken with 50-eV photons at a polar angle of $\Theta = 34^\circ$, are shown in Fig. 2. They correspond to a sampling of *k* space in an area close to the border of the BZ of pristine graphite. Note that the HOPG sample is characterized by in-plane disorder of monocrystalline grains, the area of which does not exceed the size of the photon beam. Thus the measured angle-resolved PE signals were averaged over all azimuthal angles. The bottom spectrum (a), taken for the clean

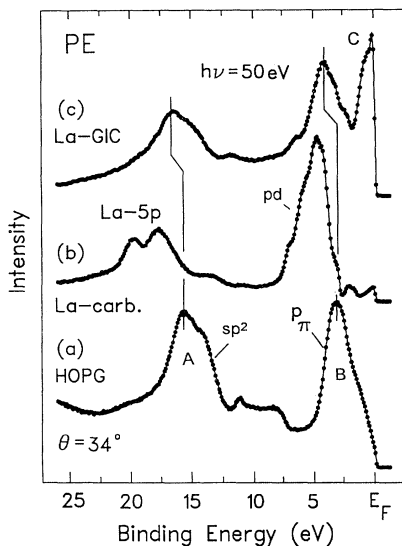


FIG. 2. Angle-resolved photoemission spectra of (a) HOPG, (b) an ordered phase of La-carbide, and (c) La-intercalated HOPG taken with a photon energy of 50 eV and at a polar angle of $\Theta = 34^\circ$; this corresponds to a *k* value close to the border of the BZ of graphite.

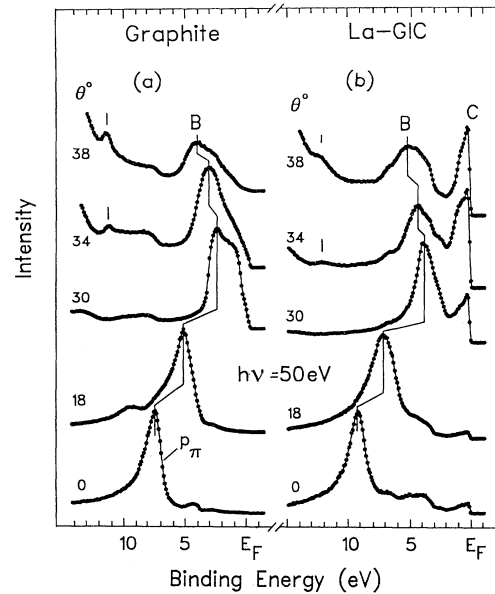


FIG. 3. Angle-resolved photoemission spectra taken with 50-eV photons for various polar angles Θ : (a) HOPG; (b) La-intercalated HOPG.

HOPG substrate, contains two main structures *A* and *B* that are separated from each other by a spectral region with rather low intensity. The shape of this spectrum is in agreement with data presented in other photoemission studies of graphite.^{27,28} According to band-structure calculations for pristine graphite,²⁹ the low-binding-energy (BE) structure *B* can be assigned to p_{π} states, which follow an almost 6-eV dispersion toward E_F when going from the Γ point to the border of the BZ (see Fig. 3). The other dispersive broad structure *A* in the region between 13- and 17-eV binding energy originates from sp^2 hybrid states.

The angle-resolved PE spectra for the ordered phase, obtained after annealing the La-C system at a temperature of 900 °C, look completely different from those obtained for pure HOPG. The sp^2 feature *A* is no longer observed in the center spectrum of Fig. 2. Instead, a La 5*p* core-level signal appears in this energy region. In contrast to HOPG, the main feature in the low-binding-energy region (at ≈ 6 -eV BE) does not show a noticeable dispersion when the polar angle is changed. In addition, two other low-intensity structures can be distinguished: a peak at about 2-eV BE and a triangle-like structure at the Fermi level. The shape of the discussed spectrum is similar to the structure of PE spectra taken for carbides of *d* transition metals with a main *pd* hybrid feature located in the region of ≈ 5 -eV BE.³⁰

Further annealing at a temperature of ≈ 1200 °C leads to a reappearance of structures *A* and *B*, which originate from sp^2 and p_{π} orbitals, respectively. Both of these structures are shifted by 1.2 eV to higher binding energies. The La 5*p* intensity decreases; in addition, it is superimposed by a pronounced sp^2 feature. The main difference, however, between the bottom and the upper

spectra in Fig. 2 is an intense feature *C*, which is characterized by a narrow peak directly at the Fermi level; it is only present in the upper spectrum taken for the La-GIC compound. This peak is in agreement with AES data that reveal the appearance of the corresponding 281-eV feature in the $C(KVV)$ AES spectrum of La-GIC (Fig. 1). The upper angle-resolved PE spectrum in Fig. 2 is very similar to those for alkali-GIC's taken in the region of the *K* point in reciprocal space. Thus, following Refs. 7 and 31, we assign the Fermi-level peak *C* to carbon-derived electronic states, which were unoccupied in pristine graphite. Within the rigid-band approximation, these states shift to lower energies and are then filled in the GIC due to charge transfer of valence electrons from La.

A set of angle-resolved PE spectra for the surface phase of La-GIC, taken with $h\nu=50$ eV at various polar angles, is shown in Fig. 3(b), in comparison with corresponding spectra for the clean HOPG substrate [see Fig. 3(a)]. The angle-resolved PE spectra for pristine HOPG are in agreement with the experimental results of Ref. 27 as well as with the results of band-structure calculations.³² The normal-emission spectrum gives no indication of electronic states at E_F in the Γ -point region of the graphite BZ. As has already been discussed, the main feature *B* stems from p_π electronic states, which are characterized by a strong dispersion toward E_F when going from the Γ point to the border of the Brillouin zone. These states are responsible for the conductivity in semimetallic graphite.

Except for the low-binding-energy region, the PE spectra for La-GIC look almost identical to the spectra obtained for pyrolytic graphite; however, they are shifted to higher energies by 1.2–1.4 eV depending on the sampling point in the BZ. As in the case of HOPG, feature *B*, which corresponds to p_π electronic states, exhibits an almost 6-eV dispersion toward E_F ; it reaches a position closest to E_F at the border of the Brillouin zone of the nonreconstructed surface. The similarity of the PE spectra of HOPG and La-GIC is really striking. Not only the main feature *B* is duplicated, but also some of the finer details (marked by vertical bars in Fig. 3). Note that despite a surface reconstruction observed by scanning tunneling microscopy (STM) (Ref. 20) and LEED, the additional back-folded features are not clearly monitored by the angle-resolved PE spectra of La-GIC.

In addition to the structures already discussed, a sharp asymmetric feature develops at the Fermi level in the spectra of the La-GIC when the polar angle Θ is increased. The PE weight of this feature is low for small angles; it is of the same order of magnitude as the intensity of features observed in the same energy region for the carbide phase (Fig. 2, center spectrum). On the other hand, this structure is most intense in the spectrum taken at an angle that corresponds to emission from the border of the BZ. It consists of a sharp peak directly at the Fermi level and a shoulder at a binding energy of 1 eV. The inset in Fig. 4 shows the dependence of the intensity of this Fermi-level peak on the angle Θ . The signals are normalized to equal photon flux, assuming a cosine law for the dependence of the intensity on the angle between the electric-field vector of the linearly polarized synchro-

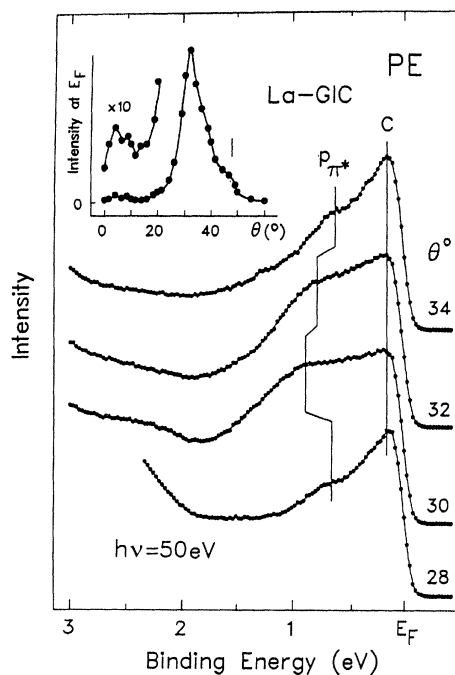


FIG. 4. Angle-resolved valence-band photoemission spectra of La-GIC recorded with 50-eV photons from the region close to the border of the BZ of graphite. The inset gives the signal weight at the Fermi level as a function of Θ .

tron radiation and the direction of electron detection. The intensity grows by a factor of almost 50 close to the border of BZ (at $\Theta \approx 32^\circ$) as compared to the value at the Γ point. Note also a fine structure of this angular dependence: a weakly pronounced peak at $\Theta \approx 7^\circ$ (magnified ten times in the inset of Fig. 4) and a shoulder at an angle of 48° (marked by a solid vertical bar).

Angle-resolved PE spectra from the binding-energy region close to the Fermi level are presented in Fig. 4; they were measured from the region at the border of the BZ ($\Theta=28^\circ$ – 34°). The PE weight there is built up by the two structures discussed above, which behave differently when the polar angle is changed. The shoulder shows a 0.2-eV dispersion to the high-binding-energy side when going from 28° to 30° (first BZ). For larger angles (second BZ), it disperses back to the low-binding-energy region. Its relative intensity is maximal at the border of the BZ. In contrast to the high-binding-energy shoulder, peak *C*, which is located directly at E_F , does not show a dispersion with the angle Θ .

DISCUSSION

Based on the angle-resolved PE, AES, and LEED results presented and discussed, the following two-step model is proposed for the incorporation of La into HOPG: In the first step, C planes are destroyed by annealing the La-HOPG interface at relatively low temperatures (400–600°C); this leads to the formation of a disordered La-C compound. Thermal annealing activates the chemical reaction between La and C, resulting in

C $2p$ –La $5d$ hybridization and in intermixing of the two components. The corresponding C(KVV) AES spectrum is similar to those observed previously for carbides [Fig. 1(b)]. Further annealing at temperatures between 800 and 900 °C leads to an ordering of the carbide phase as seen in the LEED pattern.

The PE results give strong evidence for a breaking of the in-plane graphite cells (sp^2 hybrids) and for the formation of a carbidelike compound upon annealing of the La-graphite interface at relatively low temperatures. In atomic carbon, the $2s$ and $2p$ electronic levels are at very different binding energies. This causes a large energy separation of ≈ 15 eV between the corresponding electronic states close to the Γ point in graphite. To form sp^2 hybrids, the $2s$ band and the $2p_{\sigma}$ -derived bands have to move toward each other by 7 and 8 eV, respectively; this is observed when going in k space from the center to the border of the graphitic BZ.³² The rest of the $2p$ states (with π character) show strong dispersion toward the Fermi level [see Fig. 3(a)]. On the other hand, the PE spectra of the ordered phase of La carbide (not shown here) reveal a rather weak dispersion of the valence-band electronic states (less than 1 eV) over the whole range of polar angles. The most intense peak of the $2p$ -derived electronic density of states is always located in the region between 3- and 6-eV BE (see Fig. 2, center spectrum). As a result, the $2p$ and $2s$ electronic states of carbon no longer overlap in energy. The sp^2 feature, which has been observed at a binding energy of 15 eV in HOPG (see Fig. 2, bottom), is missing in the PE spectrum of La carbide. The main contribution to covalent bonding in carbides of d transition metals stems from hybridization between the $2p$ states of C and the d states of the metal. The spectra of La carbides, obtained in the present study, are in accordance with those presented in the literature for ZrC, HfC, and TiC, with pd hybrids located at a BE between 3 and 6 eV.^{30,33}

Upon annealing of the La-HOPG interface at low temperatures, the graphite planes are destroyed in the surface region, allowing intermixing of the La and C components and, in this way, the synthesis of a surface phase of a La-carbide compound. Upon the second annealing step at high temperatures (about 1200 °C), the intermixing of La and C is intensified in a way that the surface is now enriched by carbon. The corresponding PE spectrum, measured after this high-temperature annealing step (Fig. 2, top), shows an evident decrease of the La $5p$ intensity as compared to the spectrum taken after the first low-temperature annealing step (Fig. 2, center). The concentration of La is now low, and the orienting factor of the substrate favors a recovering of the graphite planes in the surface layer. We emphasize the importance of the orienting role of the substrate, since we were not able to obtain an intercalation compound starting from amorphous carbon.

Our previous STM study²⁰ showed that after annealing step 2 the La-HOPG sample has a well-ordered structure, which shows the sixfold symmetry of the graphite layers. It is characterized, however, by longer distances between nearest-neighbor spots. Depending on the thickness of the deposited La layer and the duration of annealing,

these observations point to a 2×2 or $(\sqrt{3} \times \sqrt{3})R30^\circ$ (or mixed) reconstructed surface, which has also been observed for alkali-GIC.²⁵ In contrast to alkali-GIC, where STM can be performed only in a UHV setup, images of the high-temperature annealed La-HOPG interface can even be taken at atmospheric conditions. For this STM study in air, the samples were synthesized in an UHV chamber. They were characterized with AES before and after the STM measurements. Only weak traces of La oxides were detected after several minutes of scanning in air. This shows that the La atoms are trapped underneath the topmost inert layer of graphite, being strongly chemically bounded there. In addition, the large size of the trivalent La ions complicates their segregation to the surface through the hexagonal cells of carbon layers. Following the analogy in the type of reconstruction for La-GIC and alkali-GIC systems, we can estimate the surface stoichiometry to be LaC_8 and LaC_6 for the 2×2 and the $(\sqrt{3} \times \sqrt{3})R30^\circ$ reconstructed surfaces, respectively.

The angle-resolved PE spectra presented in Figs. 2 and 3 give further evidence for a recovering of the graphite-like layered structure at the surface of the high-temperature-annealed La-HOPG system. Annealing step 2 restores the PE structures A (sp^2 hybrids) and B (p_{π} orbitals), which are characteristic of pristine graphite (Fig. 2). As in the case of HOPG, the valence-band features for La-GIC show a strong dispersion upon variation of the polar angle (Fig. 3). The corresponding spectra in Fig. 3, measured for the same polar angle for HOPG and La-GIC, are almost identical, with the exception that (i) the whole PE structure for La-GIC is shifted by about 1.2–1.4 eV to higher binding energies as compared to the structure for HOPG, and (ii) a new feature C appears at the Fermi level in the PE spectrum of the La-intercalated compound. A spectral feature corresponding to the PE peak C has also been observed in the C(KVV) AES spectrum (Fig. 1, top) reflecting the carbon-derived density of states in the valence band of the La-intercalated compound. This feature, which has also been observed upon intercalation of graphite with alkali metals,^{7,31} gives strong evidence of the validity of a rigid-band picture, as well as for the strong charge transfer from La to C. Note that despite the 2×2 or $(\sqrt{3} \times \sqrt{3})R30^\circ$ reconstruction observed by LEED and STM,²⁰ almost no back-folded features can be distinguished in the valence-band PE spectrum from the La-GIC. The same conclusions have been drawn from angle-resolved PE of alkali-GIC's.³¹ This phenomenon can be explained on the basis of low PE cross sections from folded bands due to the umklapp transitions involved.

As discussed above, the calculations performed for metal-intercalated graphite [available only for alkali-GIC's (Ref. 6)] reveal a charge transfer of valence electrons from the metal to C p_{π^*} -derived two-dimensional states of graphite. Some studies claim also a charge transfer into a three-dimensional interlayer band, which is placed above E_F around the Γ point in pristine graphite.^{14,16,17} Our present PE results support the first model for the La-GIC. The main maximum in the angular dependence of the PE intensity at E_F (see the inset in Fig. 4) corresponds to a polar angle that reflects emission

from a region in reciprocal space, where the p_{π^*} -derived band crosses the border of the BZ. There is only a weak bump in the intensity variation for Θ between 5° and 8° , which can be assigned to a filled interlayer band located around the Γ point.

The model of charge transfer into nondistorted electronic states of graphite in La-GIC is also supported by the observed dispersion of the PE feature at $\cong 1$ -eV BE (see Fig. 4), which moves away from the Fermi level when proceeding toward the border of the BZ. This is in agreement with theoretical predictions for the behavior of the filled p_{π^*} band in intercalated graphite.⁶ The p_{π^*} -derived structure has its maximum intensity close to the border of the BZ, which can be explained by a pileup effect. Another feature at the Fermi level (peak C in Fig. 4) does not show any dispersion. This structure cannot be assigned to La-derived d states, because a similar sharp peak has been obtained in s -metal-intercalated graphites.⁷ Structure C does not change its relative intensity with time and therefore can also not be assigned to a surface state. This structure could well be the tail of a dispersive p unoccupied state,^{6,32} which is simply cut by

the Fermi edge. An inverse photoemission study could clarify the origin of this structure. Note that feature C is most pronounced on both sides of the border of the non-reconstructed BZ ($\Theta=24^\circ-28^\circ$ and $34^\circ-38^\circ$), where the p_{π^*} -derived bands are supposed to cross E_F . This is the condition for a charge-density wave, which are expected to exist in one- or two-dimensional systems.^{34,35} The origin of feature C is not clear at the present time; further studies are in progress in our laboratories.

ACKNOWLEDGMENTS

The work was supported by the Bundesminister für Forschung und Technologie, Project No. 05-5KEAXI-3/TP01, and the Sonderforschungsbereich-290, TPA06, of the Deutsche Forschungsgemeinschaft, as well as by the Scientific-Technical Program "Fullerenes and Atomic Clusters" of the Russian Ministry of Science and Technology. Four of the authors (A.M.S., S.L.M., G.V.P., and V.K.A.) thank the Freie Universität Berlin for financial support and hospitality.

*On leave from Institute of Physics, St. Petersburg State University, 198904 St. Petersburg, Russia.

†Present address: Institut für Oberflächen- und Mikrostrukturphysik, Technische Universität Dresden, Mommsenstrasse 13, 01062 Dresden, Germany.

¹J. E. Fischer and T. E. Thompson, *Phys. Today* **31**(7), 36 (1978).

²U. Gubler, J. Krieg, P. Oelhafen, P. Pfluger, H. J. Güntherodt, E. Cartier, and F. Heinrich, in *Physics of Intercalation Compounds*, edited by L. Pietronero and E. Tosatti (Springer-Verlag, Berlin, 1981).

³D. P. DiVincenzo and S. Rabii, *Phys. Rev. B* **25**, 4110 (1982).

⁴G. Kaindl, J. Feldhaus, U. Ladewig, and K. H. Frank, *Phys. Rev. Lett.* **50**, 123 (1983).

⁵P. Oelhafen, P. Pfluger, E. Hauser, and H.-J. Güntherodt, *Phys. Rev. Lett.* **44**, 197 (1980).

⁶R. C. Tatar and S. Rabii, in *Extended Abstracts of the First Symposium of the Materials Research Society*, edited by P. C. Eklund, M. S. Dresselhaus, and G. Dresselhaus (Materials Research Society, Pittsburgh, 1984); R. C. Tatar, Ph.D. thesis, University of Pennsylvania, 1985.

⁷N. Gunasekara, T. Takahashi, F. Maeda, T. Sagawa, and H. Suematsu, *Z. Phys. B* **70**, 349 (1988).

⁸G. Wang, W. R. Datars, and P. K. Ummat, *Phys. Rev. B* **44**, 8294 (1991).

⁹N. B. Hannay, T. H. Geballe, B. T. Matthias, K. Andres, P. Schmidt, and D. MacNair, *Phys. Rev. Lett.* **14**, 225 (1965).

¹⁰I. T. Belash, A. D. Bronnikov, O. V. Zharikov, and A. V. Palnichenko, *Synth. Met.* **36**, 283 (1990).

¹¹T. Inoshita, K. Nakao, and H. Kamimura, *J. Phys. Soc. Jpn.* **43**, 1237 (1977).

¹²T. Ohno, K. Nakao, and H. Kamimura, *J. Phys. Soc. Jpn.* **47**, 1125 (1979).

¹³M. E. Preil and J. E. Fischer, *Phys. Rev. Lett.* **52**, 1141 (1984).

¹⁴Th. Fauster, F. J. Himpsel, J. E. Fischer, and E. W. Plummer, *Phys. Rev. Lett.* **51**, 430 (1983).

¹⁵B. Reihl, J. K. Gimzewski, J. M. Nicholls, and E. Tosatti, *Phys. Rev. B* **33**, 5770 (1986).

¹⁶D. A. Fischer, R. M. Wentzcovitch, R. G. Carr, A. Continenza, and A. J. Freeman, *Phys. Rev. B* **44**, 1427 (1991).

¹⁷M. Posternak, A. Baldereschi, A. J. Freeman, E. Wimmer, and M. Weinert, *Phys. Rev. Lett.* **50**, 761 (1983).

¹⁸M. El Makrini, D. Guerard, Ph. Lagrange, and A. Herold, *Physica B* **99**, 481 (1980).

¹⁹R. K. Mittleman, *Phys. Rev. B* **36**, 6001 (1987).

²⁰G. V. Prudnikova, A. G. Vjatin, A. V. Ermakov, A. M. Shikin, and V. K. Adamchuk, *J. Electron. Spectrosc. Relat. Phenom.* **68**, 427 (1994).

²¹A. M. Shikin, G. V. Prudnikova, A. V. Fedorov, and V. K. Adamchuk, *Surf. Sci.* **307-309**, 205 (1994).

²²A. M. Shikin, G. V. Prudnikova, and V. K. Adamchuk, *J. Electron. Spectrosc. Relat. Phenom.* **68**, 413 (1994).

²³D. E. Ramaker, *Crit. Rev. Solid State Mater. Sci.* **17**, 211 (1991).

²⁴J. M. Shulga and G. L. Gutsev, *J. Electron. Spectrosc. Relat. Phenom.* **34**, 39 (1984).

²⁵D. Anselmetti, R. Wiesendanger, and H. J. Güntherodt, *Phys. Rev. B* **39**, 11 135 (1989).

²⁶M. Laguës, D. Marchand, and C. Fretigny, *Solid State Commun.* **59**, 583 (1986).

²⁷A. R. Law, M. T. Johnson, and H. P. Hughes, *Phys. Rev. B* **34**, 4289 (1986).

²⁸I. T. McGovern, W. Eberhardt, E. W. Plummer, and J. E. Fischer, *Physica B* **99**, 415 (1980).

²⁹G. S. Painter and D. E. Ellis, *Phys. Rev. B* **1**, 4747 (1970).

³⁰H. Ihara, M. Hirabayashi, and H. Nakagawa, *Phys. Rev. B* **14**, 1707 (1976).

³¹C. Fretigny, D. Marchand, and M. Laguës, *Phys. Rev. B* **32**, 8462 (1985).

³²R. C. Tatar and S. Rabii, *Phys. Rev. B* **25**, 4126 (1982).

³³A. L. Hagström, L. I. Johansson, B. E. Jacobsson, and S. B. M. Hagström, *Solid State Commun.* **19**, 647 (1976).

³⁴K. E. Smith, G. S. Elliott, and S. D. Kevan, *Phys. Rev. B* **42**, 5385 (1990).

³⁵C. M. Varma and A. L. Simons, *Phys. Rev. Lett.* **51**, 138 (1983).